

Hammett ^{13}C NMR and X-ray studies of π -allylpalladium phosphinooxazoline chiral ligand complexes

Paul B. Armstrong,^a Lisa M. Bennett,^b Ryan N. Constantine,^a Jessica L. Fields,^a
Jerry P. Jasinski,^b Richard J. Staples^c and Richard C. Bunt^{a,*}

^aDepartment of Chemistry and Biochemistry, Middlebury College, Middlebury, VT 05753, USA

^bDepartment of Chemistry, Keene State College, Keene, NH 03435, USA

^cX-ray Crystallography Department of Chemistry and Chemical Biology, Harvard University, Cambridge, MA 02138, USA

Received 16 August 2004; revised 7 January 2005; accepted 10 January 2005

Available online 23 January 2005

Abstract—The transmission of substituent effects across the palladium center to the allyl carbons is monitored by ^{13}C NMR and X-ray crystallography as a way to probe electronic asymmetry in chiral ligand design. Based on their similar chemical shift trends and X-ray structures, the π -allylpalladium intermediates provide a good model for early transition state reactions, which are less sensitive to electronic perturbations. Hammett analysis supports an electronic basis for enantioselection that increases as the transition state becomes later.

© 2005 Elsevier Ltd. All rights reserved.

Phosphinooxazoline (PHOX) chiral ligands have proven extremely effective at inducing asymmetry in palladium-catalyzed allylic-substitution reactions.¹ These ligands are proposed to function by controlling the ratio of the *exo* to *endo* π -allylpalladium intermediates and then directing nucleophilic addition *trans* to phosphorus (the better acceptor ligand) in the favored *exo* intermediate. The low-temperature NMR structure of the initially formed alkene–palladium complex has established this ‘*trans* to phosphorus in *exo*’ addition as the major pathway.² Nonetheless, this does not preclude other explanations for its favorability (e.g., steric interactions with the nucleophile or in the product alkene complex) nor does it provide any information about the pathway(s) leading to the minor enantiomer.

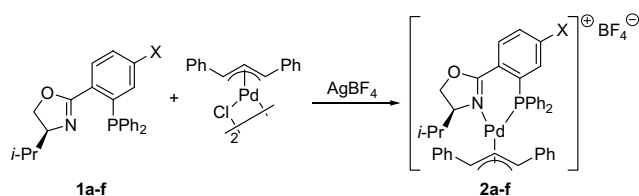
Our Hammett studies of the enantioselectivity with electronically modified PHOX ligands (**1a–f**) provided additional support for the electronic basis of the *trans* to phosphorus addition mechanism, but they also demonstrate that the nucleophile plays an important role in determining the enantioselectivity.³ In particular, for reactions with sodiodimethyl malonate as the nucleophile the ee’s were less sensitive to the backbone substituent (X) (**1a–f**: 89–93% ee). In contrast, for reactions with benzylamine as the nucleophile the ee’s showed a great sensitivity to the backbone substituent (X) (**1a–f**: 16–67% ee). These results suggest that the position of the transition state also influences the enantioselectivity.

To gain further insight into the basis for enantioselectivity and the position of the transition state, we measured the ^{13}C NMR chemical shifts and examined several X-ray structures of the π -allylpalladium intermediates themselves (**2a–f**), which are regarded as good models for an early transition state structure.⁴ ^{13}C NMR chemical shifts have been successfully correlated to both positive charge density⁵ and regioselectivity of nucleophilic attack with substituted 1,3-diphenylallylpalladium complexes with achiral ligands by Hammett analysis.⁶ In the case of ligands **1a–f** the electron donating or withdrawing substituent is on the ligand backbone and should show Hammett correlations via electronic transmission across the palladium center to the allyl termini. Based on the proposed mechanism for enantioselection, the biggest effect was expected on C₃ in the *exo* diastereomer.

Palladium complexes **2a–f** were prepared from the corresponding chiral ligands (**1a–f**)³ and 1,3-diphenylallylpalladium chloride dimer by reaction with silver tetrafluoroborate in acetone (Scheme 1).^{6b,7} The complexes were obtained in essentially quantitative yield

Keywords: Asymmetric catalysis; Hammett analysis; N,P-ligands; Palladium; π -Allyl complexes.

*Corresponding author. Tel.: +1 802 443 2559; fax: +1 802 443 2072; e-mail: rbunt@middlebury.edu



Scheme 1. Synthesis of π -allylpalladium complexes **2a–f**: X = NMe₂, OMe, Me, H, F, Cl (only *exo* diastereomer shown).

and sufficient purity for NMR spectroscopy. Analytically pure samples and crystals suitable for X-ray crystal diffraction (see below) were grown by slow vapor diffusion of diethyl ether into a solution of the complex in acetonitrile. The ¹H and ¹³C NMR assignments for **2a–f** were made based on the literature data for the analogous hexafluoroantimonate salt of **2d** (X = H)⁸ and confirmed by ¹H NMR and ¹³C HMQC NMR experiments (Table 1). The *exo:endo* ratio was determined by integration of the ¹H NMR spectra. The signals for the major diastereomer were assigned to the *exo* complex, which is known to predominate in solution.^{1a,8,9}

The ratio of *exo* to *endo* diastereomers is believed to play a role in the enantioselectivity of PHOX ligands despite their rapid equilibration in solution.^{1,10} Since nucleophilic attack *trans* to phosphorus in the *endo* complex gives the opposite (minor) enantiomer and would, presumably, also be electronically favored, this pathway must be disfavored by some other means. A change in the *exo:endo* ratio as a function of substituent would be one possibility; however, complexes **2a–f** show a constant, approximately 6:1 *exo:endo* ratio for all the substituents investigated. Consequently, the substituent's effect on the ligand's enantioselectivity must have another origin.^{11,12}

In contrast to the *exo:endo* ratios, the chemical shifts of the allyl carbons do change with different substituents and show the expected downfield trend with electron withdrawing groups. The increased deshielding does

correlate with higher observed enantioselectivity (increasing **1a** to **1f**).³ Contrary to our expectations though, no pronounced changes in the chemical shifts of C₃ are observed in the *exo* diastereomer relative to the others; the chemical shifts of C₁ and C₃ change by about the same amount for both diastereomers. Likewise, the differences between the two allyl termini ($\Delta(\delta C_3 - \delta C_1)$) remain constant at 30.1 ppm for the *exo* complex and 20.4 ppm for the *endo* complex. The larger $\Delta\delta$ for the *exo* diastereomer has been reported in 1,3-dialkylallyl complexes of **2d** and related ligands.¹³ In addition, this $\Delta\delta$ difference has been proposed to correlate to diastereomer reactivity for several S,N- and P,N-ferrocene ligand palladium complexes.¹⁴ Therefore, it seems reasonable to conclude that the *exo* complexes of **2a–f** are either more reactive or more selective (or both) than the *endo* complexes.¹⁵ This provides an explanation for how the enantioselectivity obtained with these ligands (>98% ee in THF¹) can exceed the *exo:endo* ratio (~8:1 in THF¹²).¹⁶

These $\delta\Delta$ trends can also be seen in the similar slopes of the Hammett plots of σ_p and σ_m versus the ¹³C NMR shifts of C₁ (*trans* to N) and C₃ (*trans* to P) in both the *exo* (solid symbols) and *endo* (open symbols) complexes (Fig. 1 and 2).¹⁷ The data fits better to σ_p than σ_m , as judged by R^2 .¹⁸ The better fit to σ_p could suggest a more significant substituent influence via N; however, the uniformity of the chemical shift changes of both C₁ and C₃ indicates a similarity in the effects transmitted via N (*para* to X and *trans* to C₁) and P (*meta* to X and *trans* to C₃). Thus, the Hammett fit to σ_p is perhaps best interpreted as a general electron donating/withdrawing effect with a strong resonance component. This makes sense as the allyl fragment is π -conjugated to the ligand via Pd and σ_p is known to have a strong resonance component.¹⁷

The similarities of **2a–f** by ¹³C NMR in terms of chemical shift changes and $\Delta\delta$ led us to examine some of their X-ray structures to see if any bond length or angle differences could be detected that might explain their differing enantioselectivities. Suitable crystals were obtained for

Table 1. ¹³C NMR chemical shifts of π -allylpalladium complexes **2a–f**

X	<i>exo:endo</i> ^a	Exo			Endo		
		C ₁ (<i>exo</i>)	C ₃ (<i>exo</i>)	$\Delta\delta^b$ (<i>exo</i>)	C ₁ (<i>endo</i>)	C ₃ (<i>endo</i>)	$\Delta\delta^b$ (<i>endo</i>)
NMe ₂	85:15	69.87	100.03	30.16	73.91	94.22	20.31
OMe	86:14	70.57	100.65	30.08	74.62	95.02	20.40
Me	85:15	70.58	100.80	30.22	74.61	95.18	20.57
H	86:14	70.74	100.85	30.11	74.73	95.14	20.41
F	86:14	71.19	101.26	30.07	75.32	95.63	20.31
Cl	83:17	71.28	101.26	29.98	75.32	95.81	20.49

^a Ratio determined by integration of ¹H NMR spectra taken in CD₂Cl₂ and based on the average of all resolved peaks for each complex.

^b $\Delta\delta = \delta C_3 - \delta C_1$.

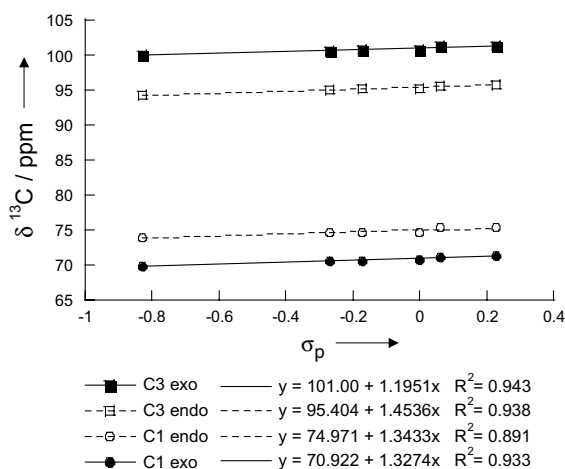


Figure 1. Hammett plot of $\delta^{13}\text{C}$ versus σ_p for complexes **2a–f**.

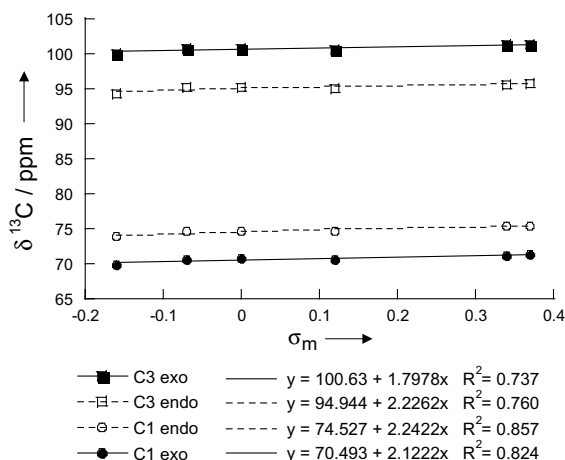


Figure 2. Hammett plot of $\delta^{13}\text{C}$ versus σ_m for complexes **2a–f**.

one electron donating complex (ent-**2b**, X = OMe) and one electron withdrawing complex (**2f**, X = Cl). Their structures were solved¹⁹ and ORTEP plots²⁰ are shown in Figures 3 and 4. Key structural parameters are com-

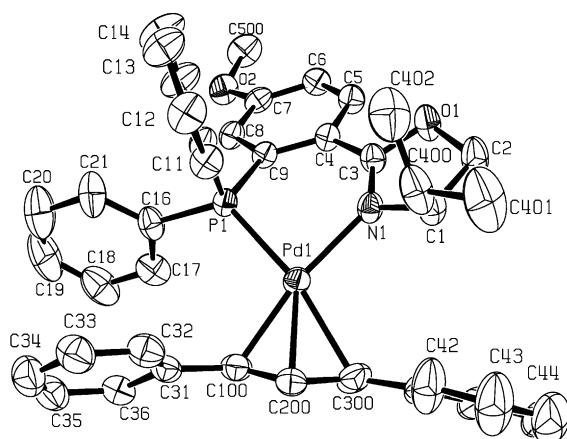


Figure 3. ORTEP drawing (30% ellipsoids) of ent-**2b** (enantiomer of ligand **1b** was used for crystal structure of **2b**) with hydrogens and BF_4^- anion omitted for clarity.

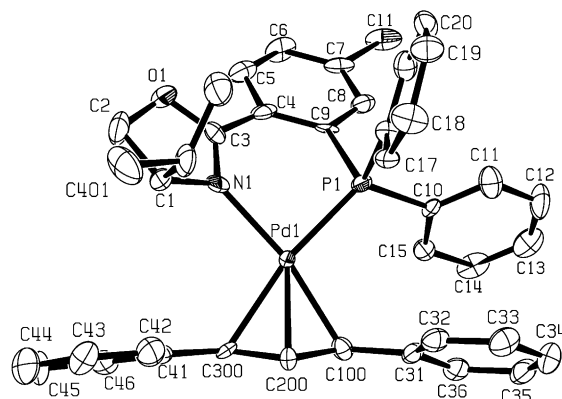


Figure 4. ORTEP drawing (40% ellipsoids) of **2f** with the hydrogens and BF_4^- omitted for clarity.

pared with the known structure of **2d**⁸ (Table 2). While some variation in bond lengths and angles between the three structures are apparent, no striking differences were found that suggest any structural basis for the substituent effects. In addition, small perturbations in twist angle (τ) and other ligand and allyl conformations have been attributed to crystal packing forces.⁸ Thus, it seems that by NMR and X-ray crystallography these allylpalladium complexes are remarkably similar despite the differences obtained with the ligands in some asymmetric reactions.

Based on the similarity of both the ^{13}C NMR data and the X-ray structure data for the allylpalladium complexes, very little difference in enantioselectivity is expected with ligands **1a–f** for reactions proceeding through an early transition state. This is precisely what was observed for reactions with sodiodimethyl malonate as the nucleophile.³ In contrast, reactions with benzylamine as the nucleophile in which large differences in enantioselectivity were observed with ligands **1a–f** likely proceed through a later transition state. With more bond formation between the nucleophile and C_3 (for the major enantiomer via *exo* diastereomer) in a later transition state, the palladium–ligand complex accepts more electron density back from the allyl fragment as it rotates to form the palladium(0)–alkene complex. The ability of the ligand (presumably primarily through

Table 2. Selected bond distances and angles from the X-ray crystal structures of **2b,d,f**

Parameter	2b (X = OMe)	2d (X = H) ^a	2f (X = Cl)
Pd–C ₁ distance (Å)	2.142(4)	2.137(2)	2.16(1)
Pd–C ₃ distance (Å)	2.288(4)	2.258(2)	2.250(11)
Pd–N distance (Å)	2.113(4)	2.096(2)	2.111(9)
Pd–P distance (Å)	2.2828(9)	2.2668(5)	2.285(3)
N–Pd–P (°)	87.46(9)	88.92(5)	87.3(3)
C ₁ –Pd–C ₃ (°)	65.76(19)	66.75(8)	65.6(4)
Tilt angle, α (°) ^b	113.9	118.5	115.0
Twist angle, τ (°) ^c	5.5	5.3	3.0

^a Data for complex **2d** (SbF_6^- salt) taken from Ref. 8.

^b Tilt angle defined between the [N, Pd, P] and [C₁, C₂, C₃] planes.

^c Twist angle defined as dihedral [N, P, C₁, C₃].

phosphorus) to accept this electron density must then be modulated by the substituents (X).

Combined with the increased reactivity or selectivity of the *exo* complex ($\Delta\delta = 30.1$ ppm vs 20.4 ppm for *endo*), the variable position of the transition state provides a general explanation for the electronic basis for enantioselection. The *exo* complex either reacts faster (*trans* to P) or more selectively (*trans* to P vs *trans* to N) than the *endo* complex.¹⁵ This inherent bias is not easily perturbed by the backbone substituents (X) for reactions with early transition states as the similar trends in the ¹³C NMR chemical shifts and X-ray structures show. Surprisingly, these results suggest that as the reaction coordinate shifts toward a later transition state, where steric effects are often invoked to explain enantioselectivity, the electronic perturbations become more important, not less. These electronic effects may be superimposed on any underlying steric influences though.

In summary, despite the potential for ligands **1a–f** to show different enantioselectivity, their 1,3-diphenylallyl-palladium complexes (**2a–f**) show similar trends in their ¹³C NMR chemical shifts and complexes **2b,d,f** have strikingly similar X-ray crystal structures. Hammett analysis suggests a general correlation with the resonance acceptor/donor ability of the substituent (via fit to σ_p). Thus, we conclude that reactions which show enantiomeric variation with ligands **1a–f** proceed by a transition state that is later relative to the allylpalladium intermediates. With this better understanding of the electronic basis for enantioselection with PHOX ligands, the design of new chiral ligands of this and other types, as well, should be greatly improved. We are continuing our investigations of these ligands by synthesizing isomeric 5-substituted PHOX ligands to better understand the Hammett analysis of σ_m and σ_p and the influence of the substituent position.

Acknowledgements

This research was supported by an award from Research Corporation, and acknowledgment is also made to the Donors of The Petroleum Research Fund, administered by the American Chemical Society, for support of this research.

Supplementary data

Supplementary data associated with this article can be found, in the online version, at [doi:10.1016/j.tetlet.2005.01.032](https://doi.org/10.1016/j.tetlet.2005.01.032). Synthesis and characterization data for **1c** and **2a–c,e–f** can be found, in the online version.

References and notes

- (a) Helmchen, G.; Pfaltz, A. *Acc. Chem. Res.* **2000**, *33*, 336–345; (b) Helmchen, G. *J. Organomet. Chem.* **1999**, *576*, 203–214; (c) Williams, J. M. J. *Synlett* **1996**, 705–710.
- (a) Junker, J.; Reif, B.; Junker, B.; Felli, I. C.; Reggeline, M.; Griesinger, C. *Chem. Eur. J.* **2000**, *6*, 3281–3286; (b) Steinhagen, H.; Reggeline, M.; Helmchen, G. *Angew. Chem., Int. Ed.* **1997**, *36*, 2108–2110.
- Constantine, R. N.; Kim, N.; Bunt, R. C. *Org. Lett.* **2003**, *5*, 2279–2282.
- Auburn, P. R.; Mackenzie, P. B.; Bosnich, B. *J. Am. Chem. Soc.* **1985**, *107*, 2033–2046.
- Akermark, B.; Krakenbergen, B.; Hansson, S.; Vitagliano, A. *Organometallics* **1987**, *6*, 620–628.
- (a) Branchadell, V.; Moreno-Manas, M.; Pajuelo, F.; Pleixats, R. *Organometallics* **1999**, *18*, 4934–4941; (b) Moreno-Manas, M.; Pajuelo, F.; Parella, T.; Pleixats, R. *Organometallics* **1997**, *16*, 205–209; (c) Malet, R.; Moreno-Manas, M.; Parella, T.; Pleixats, R. *J. Org. Chem.* **1996**, *61*, 758–763.
- See [Supplementary material](#) for experimental procedures and full characterization data.
- Kollmar, M.; Steinhagen, H.; Janssen, J.; Goldfuss, B.; Malinovskaya, S. A.; Vazquez, J.; Rominger, F.; Helmchen, G. *Chem. Eur. J.* **2002**, *8*, 3103–3114.
- Baltzer, N.; Macko, L.; Schaffner, S.; Zehnder, M. *Helv. Chim. Acta* **1996**, *79*, 803–812.
- Kudis, S.; Helmchen, G. *Angew. Chem., Int. Ed.* **1998**, *37*, 3047–3050.
- The *exo:endo* ratio for the chloro-substituted complex (**2f**) was determined from only two resolved peaks to due to increased spectral overlap (data not shown). Furthermore, the 83:17 ratio is not statistically different (based on a standard deviation of the average of 2.0%) from the other ratios.
- The *exo:endo* ratio is solvent dependent and has been reported as 8:1 in THF-*d*₈, 11:1 in DMSO-*d*₆, and 6:1 in CDCl₃ see Refs. [1](#) and [8](#).
- Kollmar, M.; Goldfuss, B.; Reggeline, M.; Rominger, F.; Helmchen, G. *Chem. Eur. J.* **2001**, *7*, 4913–4927.
- (a) You, S. L.; Hou, X. L.; Dai, L. X.; Yu, Y. H.; Xia, W.; Sun, J. *J. Org. Chem.* **2002**, *67*, 4684–4695; (b) Deng, W. P.; You, S. L.; Hou, X. L.; Dai, L. X.; Yu, Y. H.; Xia, W. *J. Am. Chem. Soc.* **2001**, *123*, 6508–6519.
- The pathway leading to the minor enantiomer is not known. If the preference for nucleophilic attack *trans* to phosphorus is essentially complete as suggested by work with unsymmetrical allyl substrates (see Ref. [8](#)), then it becomes an issue of reactivity alone (*exo* vs *endo*) rather than selectivity (attack *trans* to N vs P).
- The difference in $\delta\Delta$ between the *exo* and *endo* diastereomers is likely the result of steric interactions between the allyl substituent and the equatorial phenyl ring on phosphorus that result in a decreased influence of the *trans* effect in the *endo* complex. In complexes of **1a–f** with an unsubstituted allyl fragment lacking these steric interactions the *endo* complex is favored (55–60%) in solution and shows a greater $\delta\Delta$ in the ¹³C NMR shifts than the minor *exo* complex (24 ppm vs 18 ppm). For similar examples see Ref. [9](#).
- Substituent constants (σ_p and σ_m) taken from: Hansch, C.; Leo, A.; Taft, R. W. *Chem. Rev.* **1991**, *91*, 165–195.
- Analysis with dual-parameter equations (e.g., F/R , σ_p/σ_R , etc.) gave slightly better fits ($R^2 > 0.96$, data not shown) as would be expected with an added degree of freedom but provided no additional insights.
- CCDC-239501 (**2b**) and CCDC-239500 (**2f**) contain the supplementary crystallographic data for this paper. These data can be obtained free of charge via http://www.ccdc.cam.ac.uk/data_request/cif, or by emailing data_request@ccdc.cam.ac.uk, or by contacting The Cambridge Crystallographic Data Centre, 12, Union Road, Cambridge CB2 1EZ, UK; fax: +44 1223 336033. Com-

pound **2b**: crystallized from CH₃CN/Et₂O, colorless prisms 0.50 × 0.52 × 0.52 mm, tetragonal, space group *P*4₁2₁2, *a* = 13.6171(9), *b* = 13.6208(9), *c* = 42.281(2) Å, $\alpha = 90^\circ$, $\beta = 90^\circ$, $\gamma = 90^\circ$, *V* = 7842.2(8) Å³, *Z* = 8, $\rho_{\text{calcd}} = 1.40 \text{ g cm}^{-3}$, $2\theta_{\text{max}} = 60.82^\circ$, Mo K α radiation ($\lambda = 0.710730 \text{ Å}$, graphite monochromoter), Θ scan, *T* = 294 K, 12,907 reflections collected, 11,888 independent reflections, 7371 reflections [*I* > 2 σ (*I*)], $\mu = 0.570 \text{ mm}^{-1}$, *T*_{max}/*T*_{min} = 0.75/0.74, 474 refined parameters, hydrogen atoms placed geometrically after each cycle, *R* = 0.047, *R*_w = 0.052, refinement on |*F*|, residual electron density −0.80(1.02) e[−] Å^{−3}. Compound **2f**: crystallized from CH₃CN/Et₂O, white prisms 0.50 × 0.52 × 0.52 mm, orthorhombic, space group *P*2₁2₁2₁, *a* = 13.679(6), *b* = 13.766(7), *c* = 20.76(1) Å, $\alpha = 90^\circ$, $\beta = 90^\circ$, $\gamma = 90^\circ$, *V* = 3908.4(31) Å³, *Z* = 4, $\rho_{\text{calcd}} = 1.41 \text{ g cm}^{-3}$, $2\theta_{\text{max}} = 55.88^\circ$, Mo K α radiation ($\lambda = 0.710730 \text{ Å}$, graphite monochromoter), 2 Θ scan,

T = 293 K, 26,154 reflections collected, 9301 independent reflections, 6061 reflections [*I* > 3 σ (*I*)], $\mu = 0.637 \text{ mm}^{-1}$, *T*_{max}/*T*_{min} = 1.00/1.00, 469 refined parameters, hydrogen atoms placed geometrically after each cycle, *R* = 0.072, *R*_w = 0.088, refinement on |*F*|, residual electron density −3.05(2.46) e[−] Å^{−3}. Programs used: structure solution: SIR92 (Altomare, A.; Cascarano, G.; Giacovazzo, G.; Guagliardi, A.; Burla, M. C.; Polidori, G.; Camalli, M. *J. Appl. Cryst.* **1994**, 27, 435), structure refinement: CRYSTALS (Watkin, D. J.; Prout, C. K.; Carruthers, J. R.; Betteridge, P. W.; Cooper, R. I. *Crystals, Issue 11*, Chemical Crystallography Laboratory, Oxford, UK, **2001**), weighting scheme: Prince modified Chebychev polynomial (Watkin, D. J. *Acta Crystallogr. Sect. A*, **1994**, 50, 411; Prince, E. *Mathematical Techniques in Crystallography and Materials Science*; Springer: New York, 1982).

20. Farrugia, L. J. *J. Appl. Crystallogr.* **1997**, 30, 565–566.